Robotica (2003) volume 21, pp. 199–210. © 2003 Cambridge University Press
DOI: 10.1017/S0263574702004691 Printed in the United Kingdom

Generating globally optimised sagittal gait cycles of a biped robot

Tarik Saidouni* and Guy Bessonnet†

(Received in Final Form: October 9, 2002)

SUMMARY

The paper is aimed at generating optimal gait cycles in the sagittal plane of a biped, the locomotion system of which has anthropomorphic characteristics. Both single and double support phases are globally optimised, considering incompletely specified transition postural configurations from one phase to the other. An impactless heel-touch is prescribed. Full dynamic models are developed for both gait phases. They are completed by specific constraints attached to the unilaterality of contact with the supporting ground.

A parametric optimisation method is implemented. The biped joint coordinates are approximated by cubic splines functions connected at uniformly distributed knots along the motion time. The finite set of unknowns consists of the joint coordinate values at knots, some gait pattern parameters at phase transitions, and the motion time of each phase. The step length is adjusted to the prescribed gait speed by the optimisation process. Numerical simulations concerning slow and fast optimal gaits are presented and discussed.

KEYWORDS: Sagittal gait; Parametric optimisation; Cubic spline interpolation; Impactless gait; Gait optimisation.

1. INTRODUCTION

The most striking characteristic of bipedal gait is certainly its intrinsic instability due to intermittent, unilateral contacts with the supporting ground. Mainly for this reason, the gait of current biped robots obeys control strategies based on dynamic stability approaches using the well-known concept of Zero-Moment Point (or ZMP).[1–4] Another matter of concern for mechanical bipeds is their walking range when considering the energy consumption. Not very well organized movements could be costly to execute. Thus, there is the need for improving the dynamics of gait in order to reduce the energy expenditure. With this aim in view, some researchers attempted to exploit the natural dynamics of bipeds so as to perform passive bipedal walking,[5–7] or to lower actuating efforts during the swing phase.[8–10] In this way, although efficient bipedal walking is necessarily active, even on level ground, it must take advantage of the natural tendency of a biped to perform as a compound pendulum system during the swing phase of gait.[10] Minimizing a suitable performance criterion defined during the gait cycle will help to generate active walk benefiting at best from the pendular effect of gravity.

Early researches on bipedal gait optimisation were focused on the single support phase (or swing phase).[10–13] In most approaches, a gait cycle consists of the single support phase followed by an instantaneous impact at the end of the swing.[12–13] The double support phase has rarely been studied as in reference [14]; it is commonly considered as instantaneous. However, the part played by the double support phase in the gait cycle is quite important to ensure an appropriate propelling effect, as well as to guarantee some continuity conditions at phase transitions, together with equilibrium recovery. Moreover, it would be interesting to evaluate its relative time length in comparison with the swing phase travelling time.

This paper is the continuation of earlier researches related to optimal gait generation of the biped BIP described in reference [15]. In previous works,[10,14] gait optimisation was performed into the frame of the optimal control theory using Pontryagin's Maximum Principle. Only the single support phase was generated in reference [10], while the two phases of gait of a five-link planar biped were optimised separately in reference [14]. In this paper, unlike former approaches, we present an algebraic optimisation method using a parameterisation technique for generating a complete gait cycle. Cubic spline functions are used to approximate generalized coordinates on time subintervals. This technique introduces a finite set of discrete optimisation parameters. It allows sub-optimal solutions to be easily computed. Spline functions are connected at points uniformly distributed along the time history. The connecting mode ensure the continuity of second derivatives, and consequently of joint accelerations at knots.

As in references [10, 14], we consider walking without impact in order to avoid destabilizing effects in controlling optimal reference gait trajectories.[16] In fact, in the present study, we go further in smoothing the biped movement by introducing continuity conditions on accelerations at gait phase transitions. In this way, actuating torques, together with reaction ground forces are continuous on the overall gait cycle. This smoother dynamics is aimed at ensuring more stable trajectory tracking by the robot controller.

The performance criterion we minimise is the time-integral of quadratic actuating torques. As during walking the biped works against gravity, the minimisation of joint actuating torques will favour upright walking together with gait benefiting from pendular effect.

We give prominence to dealing with the double support phase of gait. Since the locomotion system of the biped works as an over-actuated closed-loop mechanism, the indeterminacy of actuating torques and ground reaction

* Laboratoire de Mécanique des Structures, Ecole Polytechnique, BP17 M1, Bordj El Bahri 16111 Alger (Algeria).
E-mail: saidouni.tarik@caramail.com
† Laboratoire de Mécanique des Solides, CNRS-UMR6610, Université de Poitiers, SP2MI, Bd. M. & P. Curie, BP 30179, 86962 Futuroscope Chasseneuil cedex (France).
E-mail: bessonnet@lms.univ-poitiers.fr

forces must be solved. To that end, the method developed presents two levels of optimisation: At the first level, actuating torques are extracted as a minimal norm solution of the inverse dynamic model describing the evolution of both the torques and the ground reaction forces. In this manner, actuating torques appear as functions of generalized coordinates and their first and second derivatives. It is then possible to express the performance criterion as a function of parameters defining the generalized coordinates. Then varying the optimisation parameters can minimise, in turn, the criterion.

The paper is organized as follows: Section 2 is an overview of the method developed. In Section 3, inverse dynamic models of both gait phases are stated and solved with respect to joint actuating torques. Section 4 is devoted to the formulation of constraints specifying a feasible walk, which results in defining a maximal set of free postural and velocity parameters that are considered as complementary optimisation variables. The parameterised optimisation problem is stated in its final form in Section 5. Section 6 presents two numerical simulations that demonstrate the method developed. Finally, we describe conclusions in Section 7.

2. BASIC PRINCIPLE OF THE OPTIMISATION METHOD

For the sake of simplicity, let us consider an N-link planar kinematic chain (Figure 1), and assume that

(i) The proximal link L_1 and the distal link L_N may be or not in contact (or jointed) with a supporting base L_0.
(ii) Any motion is described by a set of n generalized coordinates q_is such as $\mathbf{q}=(q_1, \ldots, q_n)^T$, $n>N$, $\mathbf{q}$ being the configuration vector.
(iii) The mechanical system can be over-actuated; in other words, it can be subjected to m actuating inputs u_is such that $\mathbf{u}=(u_1, \ldots, u_m)^T$, with $m \geq n$.

A Lagrangian dynamic model can be expressed as an n-vector equation:

$$\mathbf{B}(\mathbf{q}, \dot{\mathbf{q}}, \ddot{\mathbf{q}})=\mathbf{A}(\mathbf{q})\mathbf{u} \tag{1}$$

where $\mathbf{B}$ is a short notation for the left hand member that has the structure

$$\mathbf{B}(\mathbf{q}, \dot{\mathbf{q}}, \ddot{\mathbf{q}}) \equiv \mathbf{M}(\mathbf{q})\ddot{\mathbf{q}}+\mathbf{C}(\mathbf{q}, \dot{\mathbf{q}})+\mathbf{G}(\mathbf{q}).$$

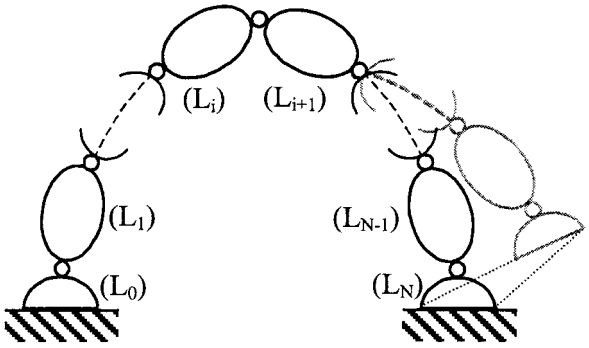

Fig. 1. Closed and open N-link kinematic chains.

In the above expressions

- $\dot{\mathbf{q}}$ (resp. $\ddot{\mathbf{q}}$) is the first-order (resp. second-order) time derivative of $\mathbf{q}$
- $\mathbf{M}$ is the mass matrix of the mechanical system in the configuration $\mathbf{q}$
- $\mathbf{C}$ regroups the Coriolis and centrifugal terms, while $\mathbf{G}$ represents the gravity terms
- In (1), $\mathbf{A}$ is a $(n \times m)$-matrix depending on $\mathbf{q}$.

Our objective is to generate an optimal motion satisfying (1) over an interval of time $[0, T]$ between two constrained end locations $\mathbf{q}(0)$, $\mathbf{q}(T)$ such that

$$\begin{cases} \mathbf{C}_0(\mathbf{q}(0))=0 \in \mathbf{R}^{n_0},\ n_0 \leq n \\ \mathbf{C}_T(\mathbf{q}(T))=0 \in \mathbf{R}^{n_T},\ n_T \leq n \end{cases}, \tag{2}$$

while minimizing the integral of quadratic inputs:

$$\text{Minimise } J,\ J=\int_0^T \mathbf{u}^T\,\mathbf{W}\,\mathbf{u}\,dt, \tag{3}$$

where $\mathbf{W}$ is a given $(m \times m)$-dimensional weighting diagonal matrix.

Conditions (3), (1), and (2) typically define an optimal control problem. We intend to restate this problem into an algebraic optimisation problem, considering a finite set of discrete optimisation variables. A general means to achieve this goal consists in representing the generalized coordinates q_is using approximation functions φ_is defined by a finite set of parameters $\mathbf{x} \in \mathbf{R}^p$ such that

$$i \leq n,\ q_i(i) \approx \varphi_i(\mathbf{x}, t). \tag{4}$$

If we set

$$\varphi=(\varphi_1, \ldots, \varphi_n)^T,\ \partial\varphi/\partial t \equiv \varphi_{,t},\ \partial^2\varphi/\partial t^2 \equiv \varphi_{,t^2}, \tag{5}$$

then Equation (1) must be satisfied with respect to $\mathbf{x}$ as follows

$$t \in [0, T],\ \mathbf{B}(\varphi(\mathbf{x}, t), \varphi_{,t}(\mathbf{x}, t), \varphi_{,t^2}(\mathbf{x}, t))=\mathbf{A}(\boldsymbol{\varphi}(\mathbf{x}, t))\,\mathbf{u}(t). \tag{6}$$

In order to minimise J in (3), the vector $\mathbf{u}$ of actuating inputs must be explicitly formulated as a vector-function of $\mathbf{x}$ and t by solving in $\mathbf{u}$ the linear algebraic system (6). A special attention is devoted to this solving operation in the next section. Assuming that this computing process is achieved, the vector-function $\mathbf{u}$ can be formally written as

$$\mathbf{u}(t)=\mathbf{U}(\mathbf{x}, t) \equiv \mathbf{U}(\varphi(\mathbf{x}, t), \varphi_{,t}(\mathbf{x}, t), \varphi_{,t^2}(\mathbf{x}, t)). \tag{7}$$

In this way, the cost J can be expressed as the following function of $\mathbf{x}$

$$J(\mathbf{x})=\int_0^T \mathbf{U}^T(\mathbf{x}, t)\,\mathbf{W}\,\mathbf{U}(\mathbf{x}, t)\,dt. \tag{8}$$

In the same way, constraints (2) can be reformulated in $\mathbf{x}$ into the form

$$\begin{cases} \mathbf{C}_0(\varphi(\mathbf{x}, 0))=0 \\ \mathbf{C}_T(\varphi(\mathbf{x}, T))=0 \end{cases}. \tag{9}$$

https://doi.org/10.1017/S0263574702004691 Published online by Cambridge University Press

Through (4), (6), and (7), the optimal control problem (1), (2), (3) is thus reduced to the constrained optimisation problem (8), (9) which consists in minimizing the function $J(\mathbf{x})$ depending on the finite set of discrete variables x_is in $\mathbf{x}$, while satisfying the equality constraints (9).

3. DYNAMIC MODELS

During the gait cycle, the biped performs as a varying kinematic structure due to the fact that double support phases alternate with single support ones. During the double support phase (DS-phase or bipodal phase), both feet are in contact with the supporting ground and the locomotion system works as an over-actuated close kinematic chain. In this case, movements generated must avoid undesirable antagonistic efforts in the mechanical structure that could provoke destabilizing effects, such as a break in the ground-foot contact or sliding. During the single support phase (SS-phase, or unipodal, or swing phase) the biped moves as a rooted tree-like mechanical system. Motions must be organized in order to avoid ground collision together with a heel-strike of the swing foot. Dynamics of each above main phases of gait call for specific modelling.

3.1. Double support phase model

Figure 2 shows initial and final postural configurations of the DS-phase of the planar biped. At the beginning of the bipodal phase, the rear foot is flat on the ground, and the front foot is in contact at heel level. We assume that during the whole phase, both feet are pivoting in the vertical plane, the first, round its tip, and the second, round its heel. This phase ends as soon as the front foot is flat on the ground. The locomotion system is then kinematically equivalent to a seven-bar mechanism.

Dynamic equations of such a constrained mechanism can be derived by opening the kinematic loop, and by using Lagrange's multipliers. We make use of this technique in a more radical manner, by considering the biped freed from its two ground contacts (Figure 3). This approach enables the contact forces to be directly integrated into the Lagrangian dynamic model. In fact, we will consider such

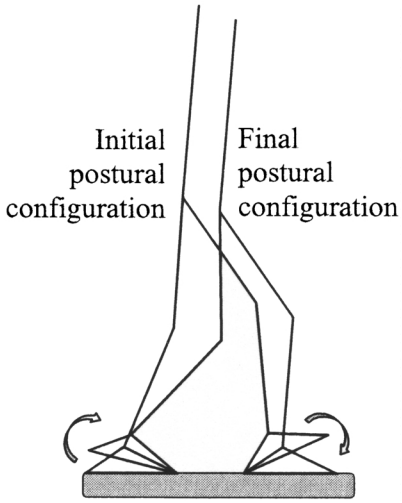

Fig. 2. Biped configurations at beginning and at end of the DS-phase.

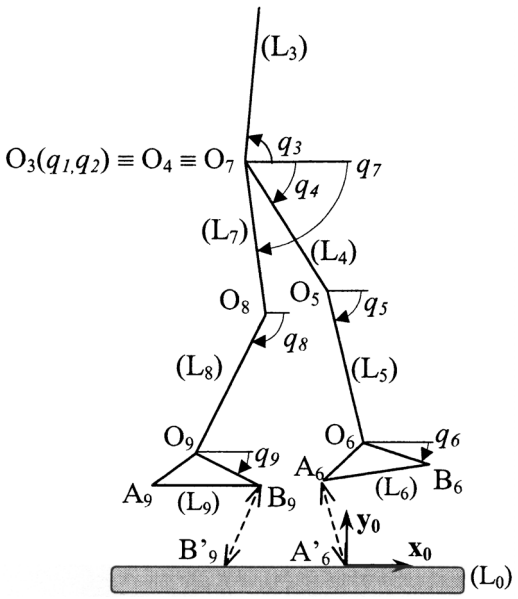

Fig. 3. Flying kinematic model of a seven-link planar biped.

forces as unknown external forces to be applied in order to keep the tip of the rear foot, and the heel of the front foot, in their assigned contact positions.

Considering the biped as a free system, we define a vector $\mathbf{q}$ of generalized coordinates comprising the Cartesian coordinates q_1 and q_2 of the hip, together with the absolute joint rotations q_3 to q_9 of the seven links numbered from 3 to 9 (Figure 3), thus $\mathbf{q}=(q_1, \ldots, q_9)^T$.

Closure conditions are defined as

$$\begin{cases} \phi_R(\mathbf{q}) \equiv \overline{B_9 B'_9}(q_1, q_2, q_7, q_8, q_9) = 0 \in \mathbf{R}^2 \\ \phi_F(\mathbf{q}) \equiv \overline{A_6 A'_6}(q_1, q_2, q_4, q_5, q_6) = 0 \in \mathbf{R}^2 \end{cases} \tag{10}$$

where ϕ_R (resp. ϕ_F) is related to the rear (resp. front) foot.

The force $\mathbf{F}_R$ applied at the tip of the rear foot, and the force $\mathbf{F}_F$ applied at the heel of the front foot can be projected as follows:

$$\begin{cases} \mathbf{F}_R = F_{R,x}\mathbf{x}_0 + F_{R,y}\mathbf{y}_0 \\ \mathbf{F}_F = F_{F,x}\mathbf{x}_0 + F_{F,y}\mathbf{y}_0 \end{cases}. \tag{11}$$

Using the above notations, motion equations may be written in the following form:

$$\mathbf{M}(\mathbf{q})\ddot{\mathbf{q}} + \mathbf{C}(\mathbf{q}, \dot{\mathbf{q}}) + \mathbf{G}(\mathbf{q}) = \mathbf{D}\mathbf{u} + \mathbf{J}_R^T\mathbf{F}_R + \mathbf{J}_F^T\mathbf{F}_F \tag{12}$$

where $\mathbf{J}_R$ (resp. $\mathbf{J}_F$) is the Jacobian matrix of ϕ_R (resp. ϕ_F), $\mathbf{D}$ is the control input matrix and $\mathbf{u}$ is the 6-order vector of joint actuating torques.

Considering all active forces $\mathbf{u}$, $\mathbf{F}_R$ and $\mathbf{F}_F$ as unknown actuating inputs, and setting

$$\mathbf{u}^{*T} = (\mathbf{u}^T, \mathbf{F}_R^T, \mathbf{F}_F^T). \tag{13}$$

equation (12) can be concisely expressed under the form (1), that is

$$\mathbf{B}(\mathbf{q}, \dot{\mathbf{q}}, \ddot{\mathbf{q}}) = \mathbf{A}(\mathbf{q})\mathbf{u}^* \tag{14}$$

where $\mathbf{A}$ is the (9×10)-dimensional control input matrix defined as the concatenation of three matrices, namely

$$\mathbf{A} = (\mathbf{D}, \mathbf{J}_R^T, \mathbf{J}_F^T). \tag{15}$$

https://doi.org/10.1017/S0263574702004691 Published online by Cambridge University Press

Following the general method described in Section 2, we need to solve (14) with respect to $\mathbf{u}^*$. This linear system is underdetermined (there are 10 unknowns for 9 independent equations). The approach we put forward consists in extracting a minimal quadratic-norm solution. The matrix $\mathbf{A}$ having full rank, this operation can be achieved using the right pseudo-inverse matrix $\mathbf{A}_R^+$ of $\mathbf{A}$ such that (see, for instance, reference [17]):

$$\mathbf{A}_R^+ = \mathbf{A}^T(\mathbf{A}\mathbf{A}^T)^{-1}.$$

Then, among the infinity of solutions to the underdetermined system (14), an optimal one in term of minimal norm of $\mathbf{u}^*$ is given by the following expression

$$\mathbf{u}^*(\mathbf{q}, \dot{\mathbf{q}}, \ddot{\mathbf{q}}) \equiv \begin{pmatrix} \mathbf{u}(\mathbf{q}, \dot{\mathbf{q}}, \ddot{\mathbf{q}}) \\ \mathbf{F}_R(\mathbf{q}, \dot{\mathbf{q}}, \ddot{\mathbf{q}}) \\ \mathbf{F}_F(\mathbf{q}, \dot{\mathbf{q}}, \ddot{\mathbf{q}}) \end{pmatrix} = \mathbf{A}_R^+(\mathbf{q})\mathbf{B}(\mathbf{q}, \dot{\mathbf{q}}, \ddot{\mathbf{q}}). \quad (16)$$

Recall that we intend to use the expression of $\mathbf{u}$ taken from (16) to formulate the integral of the cost function J in (3). Also note that $\mathbf{u}^*$ and $\mathbf{q}$ in (16) satisfy the Equation (14). But, in addition, $\mathbf{q}$ must satisfy the closure constraints (10). These conditions will be fulfilled by minimizing their quadratic residual values, using the penalty function

$$\Phi(\mathbf{q}) = r_R(\phi_R(\mathbf{q}))^2 + r_F(\phi_F(\mathbf{q}))^2, \quad (17)$$

to be introduced in the integral cost J, the integrand of which becoming a function of $\mathbf{q}$, $\dot{\mathbf{q}}$, $\ddot{\mathbf{q}}$:

$$J = \int_0^T [\mathbf{u}^T(\mathbf{q}, \dot{\mathbf{q}}, \ddot{\mathbf{q}})\, \mathbf{W}\, \mathbf{u}(\mathbf{q}, \dot{\mathbf{q}}, \ddot{\mathbf{q}}) + \Phi(\mathbf{q})]\, dt. \quad (18)$$

Also recall that the q_is in $\mathbf{q}$ will be replaced by functions of type (4), in Section 5.

3.2. Single support phase model

The single support phase, or swing phase, begins at the toe-off of the rear foot and ends at heel-touch. During the swing, we assume that the stance foot stays flat on the ground (Figure 4) implying that $q_6 = \alpha$, a constant value. As a consequence, the kinematics of the biped can be described by only 6 independent joint variables such as

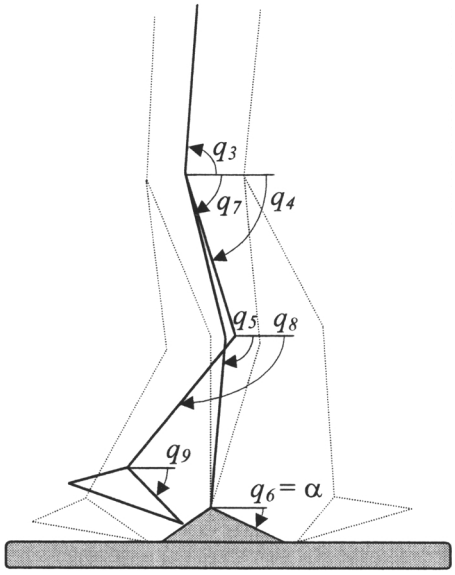

Fig. 4. Kinematic model of the single-support phase.

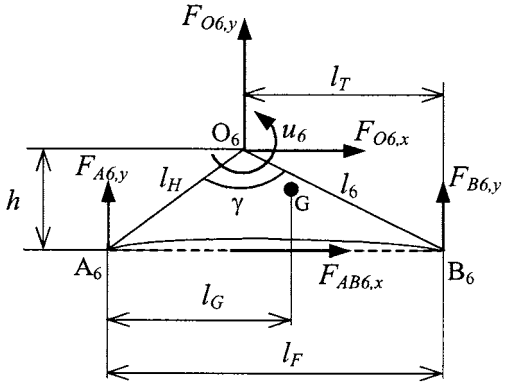

Fig. 5. Contact forces applied on the stance foot, and interaction forces at the ankle.

$$\mathbf{q}^* = (q_3, q_4, q_5, q_7, q_8, q_9)^T. \quad (19)$$

Moreover, since the biped moves as an open kinematic chain, there is no indeterminacy in computing the ground-foot contact forces. Thus, we can use explicitly the reduced joint-coordinate configuration (19) in order to decrease the complexity of the dynamic model.

On the other hand, the contact forces of the stance foot with the ground may be modelled using two normal forces $F_{A6,y}$ and $F_{B6,y}$ applied at end points of the sole, together with a horizontal force $F_{AB6,x}$ acting along the AB axis (Figure 5). This system of forces may be equivalently considered as the actuating torque u_6, and the forces $F_{O6,x}$ and $F_{O6,y}$ defined as:

$$F_{O6,x} = F_{AB6,x} \quad (20)$$

$$F_{O6,y} = F_{A6,y} + F_{B6,y} - M_6 g \quad (21)$$

exerted by the foot on the leg at ankle point O_6.

Then, we can adapt the formulations of the previous subsection to the configuration (19). First, using a control-force vector defined as in (13) by setting

$$\mathbf{u}^{*T} = (\mathbf{u}^T, \mathbf{F}_{O6}^T) \quad (22)$$

and noting that the B_6 component of $\mathbf{B}$ in the left hand side of Equation (14) vanishes because q_6 is constant, Equation (12) becomes

$$\mathbf{B}(\mathbf{q}, \dot{\mathbf{q}}, \ddot{\mathbf{q}}) = \mathbf{D}\mathbf{u} + \mathbf{J}_F^T(q_4, q_5)\mathbf{F}_{O6}. \quad (23)$$

Equation (23) can be expended in matrix form as in (14) such that

$$\mathbf{A}(\mathbf{q}) = \begin{pmatrix} \mathbf{0} & \mathbf{I} \\ \mathbf{D} & \mathbf{J}_F^{*T} \end{pmatrix} \quad (24)$$

where $\mathbf{J}_F^{*T}$ stands for the Jacobian matrix:

$$\mathbf{J}_F^{*T} = \frac{\partial \phi_F}{\partial \mathbf{q}^*},$$

and $\mathbf{I}$ is the 2×2 identity matrix.

Now, solving the remaining closure condition ϕ_F in (10) with respect to q_1 and q_2: $q_1 = f_1(q_4, q_5)$, $q_2 = f_2(q_4, q_5)$, it

https://doi.org/10.1017/S0263574702004691 Published online by Cambridge University Press

follows that Equation (14) can be solved in $\mathbf{FO}_6$ and $\mathbf{u}$ as functions of $\mathbf{q}^*$ and its time derivatives, that is

$$\begin{aligned} FO_{6,x} &= B_1(\mathbf{q}^*, \dot{\mathbf{q}}^*, \ddot{\mathbf{q}}^*) \\ FO_{6,y} &= B_2(\mathbf{q}^*, \dot{\mathbf{q}}^*, \ddot{\mathbf{q}}^*) \end{aligned} \tag{25}$$

$$\mathbf{u}(\mathbf{q}^*, \dot{\mathbf{q}}^*, \ddot{\mathbf{q}}^*) = \mathbf{D}^{-1} \begin{pmatrix} B_3(\mathbf{q}^*, \dot{\mathbf{q}}^*, \ddot{\mathbf{q}}^*) \\ B_4(\mathbf{q}^*, \dot{\mathbf{q}}^*, \ddot{\mathbf{q}}^*) + l_4[B_1(\mathbf{q}^*, \dot{\mathbf{q}}^*, \ddot{\mathbf{q}}^*) \sin(q_4) - B_2(\mathbf{q}^*, \dot{\mathbf{q}}^*, \ddot{\mathbf{q}}^*) \cos(q_4)] \\ B_5(\mathbf{q}^*, \dot{\mathbf{q}}^*, \ddot{\mathbf{q}}^*) + l_5[B_1(\mathbf{q}^*, \dot{\mathbf{q}}^*, \ddot{\mathbf{q}}^*) \sin(q_5) - B_2(\mathbf{q}^*, \dot{\mathbf{q}}^*, \ddot{\mathbf{q}}^*) \cos(q_5)] \\ B_7(\mathbf{q}^*, \dot{\mathbf{q}}^*, \ddot{\mathbf{q}}^*) \\ B_8(\mathbf{q}^*, \dot{\mathbf{q}}^*, \ddot{\mathbf{q}}^*) \\ B_9(\mathbf{q}^*, \dot{\mathbf{q}}^*, \ddot{\mathbf{q}}^*) \end{pmatrix} \tag{26}$$

The expression of $\mathbf{u}$ in (26) will be used like the expression of $\mathbf{u}$ in (16) to define the integrand of the cost J as a function of the q_is and their derivatives. Next, functions as the φ_is in (4) will be substituted for the q_is.

4. CONSTRAINTS DEFINING A FEASIBLE WALK

We distinguish two types of constraints a feasible step must obey.

4.1. Permanent constraints

During the gait cycle, several obvious physical conditions must be satisfied:

4.1.1. Unilaterality of contact. Vertical components of ground reaction forces must remain positive. Using notations introduced in subsections 3.1 and 3.2 together with Figure 5, these conditions can be written as

$$t \in [0, T_{DS}], \qquad F_{R,y} \geq 0,\ F_{F,y} \geq 0 \tag{27}$$

$$t \in [T_{DS}, T_{DS}+T_{SS}], \quad F_{\mathrm{A6},y} > 0,\ F_{\mathrm{B6},y} > 0, \tag{28}$$

for the DS-phase and SS-phase, respectively. T_{DS} and T_{SS} stand for the motion time of each phase. Using the notations given in Figure 5, the vertical component $F_{\mathrm{B6},y}$ is correlated during the SS-phase to both torque and force exerted at the ankle, by the relationship

$$F_{\mathrm{B6},y} = (u_6 + (l_F - l_T)F_{\mathrm{O6},y} - hF_{\mathrm{O6},x} + l_{\mathrm{G}} M_6 g)/l_F, \tag{29}$$

where M_6 is the mass of the foot (L_6), while g is the gravity acceleration. The component $F_{\mathrm{A6},y}$ is directly given by (21). Notice that through (21) and (29), constraints (28) result in limiting the ankle actuating torque u_6.

4.1.2. Actuating torque limitations. We define bounded joint actuating torques by setting

$$\forall t \in [0, T_{DS}+T_{SS}],\ |u_i(t)| \leq u_i^{\max},\ \mathrm{i} = 4, \ldots, 9. \tag{30}$$

4.1.3. Non-sliding conditions. We assume that ground-foot contacts are submitted to Coulombian friction. Non-sliding conditions must be satisfied during the DS-phase by both feet and by the stance foot during the SS-phase, namely

$$\forall t \in [0, T_{DS}],\ \begin{cases} fF_{R,y} > |F_{R,x}| \\ fF_{F,y} > |F_{F,x}| \end{cases} \tag{31}$$

$$\forall t \in [T_{DS}, T_{DS}+T_{SS}],\ f(F_{\mathrm{A6},y} + F_{\mathrm{B6},y}) > |F_{\mathrm{O6},x}| \tag{32}$$

where f is a given dry-friction coefficient.

4.1.4. Knee counter-flexion avoidance. Like during human locomotion, we assume that knees can only bend forward. Such a condition is fulfilled when the following inequalities are satisfied (see Figure 3 for the notations)

$$\forall t \in [0, T_{DS}+T_{SS}],\ \begin{cases} q_5(t) - q_4(t) < 0 \\ q_8(t) - q_7(t) < 0 \end{cases}. \tag{33}$$

4.1.5. Joint rotation bounds. Due to joint motion limitations, generalised variables are bounded as follows:

$$\forall t \in [0, T_{DS}+T_{SS}],$$
$$q_7^{\min} \leq q_7(t) - q_3(t) \leq q_7^{\max},\ q_i^{\min} \leq q_i(t) - q_{i-1}(t) \leq q_i^{\max},$$
$$i = 4, 5, 6, 8, 9. \tag{34}$$

Note that conditions (33) mean that $q_5^{\max} = q_8^{\max} = 0$.

4.1.6. Ground collision avoidance. The swing foot must not strike the ground during the SS phase. This is typically a problem of trajectory planning with collision avoidance. We define a virtual obstacle (D) that consists of a small increase in height of the ground delimited by an arc of a circle, its radius depending on the step length l_S, as shown in Figure 6. The toe and heel of the swing foot should not

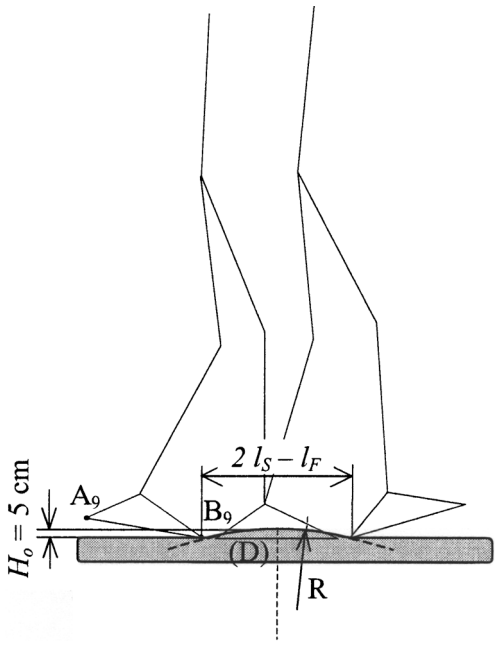

Fig. 6. Anti-collision zone for the swing phase.

https://doi.org/10.1017/S0263574702004691 Published online by Cambridge University Press

enter in collision with this obstacle: $A_9 \notin (D)$, $B_9 \notin (D)$. The anti-collision conditions may be formally written as follows:

$$\forall t \in [T_{DS}, T_{DS}+T_{SS}], \qquad \mathbf{g}(l_s, q_1, q_2, q_7, q_8, q_9) < 0. \tag{35}$$

4.2. Constraints at phase transitions

4.2.1. Definition of a gait step. We define a gait step including three boundary configurations, each one having both feet in contact with the ground (Figure 7). They correspond to phase transitions as follows:

i. An initial configuration (i) at the beginning of the DS phase, initialising the gait step.
ii. A middle configuration (m) at transition between the main two phases (end of the DS phase, beginning of the SS phase).
iii. A final configuration (f) at the end of the SS phase and beginning of the next step. If the gait is perfectly cyclic, (f) coincide with (i), the two legs being swapped.

These transition configurations are defined using non-independent generalized positions and velocities. At first, we want to select a maximal set of independent parameters to be optimised, defining completely these three configurations.

4.2.2. Maximal set of free parameters defining the transition configurations. As shown in Figure 7, the initial, middle and final postural configurations may be completely determined using the following parameters:

- The joint coordinates of the trunk: q_3^i, q_3^m.
- The joint coordinates of the front leg: q_4^i, q_5^i, q_4^m, q_5^m.
- The joint coordinate of the stance foot in configuration (i), and the swing foot in configuration (m): q_6^i, q_9^m.
- The step length: l_S.

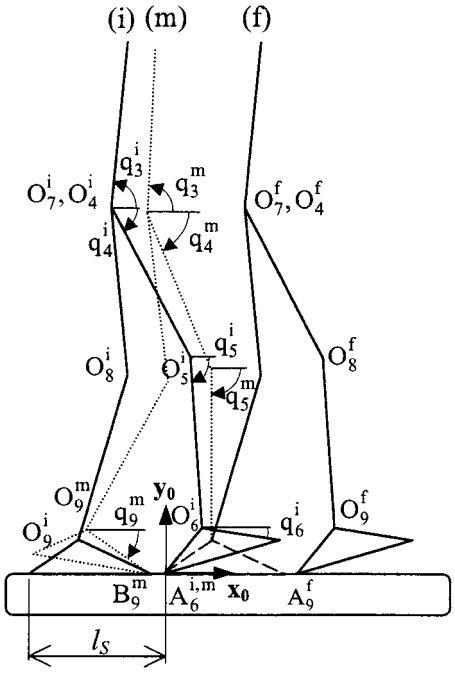

Fig. 7. The three boundary configurations of a step.

Other joint coordinates can be expressed as functions of above parameters. Firstly, as the stance foot remains flat on the ground during the SS phase, we have (Figure 4)

$$q_6^m = q_6^f = q_9^i = \alpha. \tag{36}$$

Secondly, assuming that the gait is cyclic, continuity and periodicity conditions result in the relationships (Figures 4 and 7)

$$q_3^f = q_3^i,\ q_4^f = q_7^i,\ q_5^f = q_8^i,\ q_7^f = q_4^i,\ q_8^f = q_5^i,\ q_9^f = q_6^i. \tag{37}$$

Thirdly, q_7 and q_8 can be easily computed using the double vector representation (Figure 7)

$$O_7O_9 = O_7O_8 + O_8O_9 = O_7A_9 + A_9O_9.$$

Projecting the second relationship on $\mathbf{x}_0$ and $\mathbf{y}_0$ (Figures 5, 7) gives respectively

$$\begin{aligned} l_7 \cos(q_7) + l_8 \cos(q_8) &= -q_1 + l_F - l_S - l_6 \cos(q_9) \\ l_7 \sin(q_7) + l_8 \sin(q_8) &= -q_2 - l_6 \sin(q_9) \end{aligned} \tag{38}$$

where the hip coordinates q_1 and q_2, during the gait cycle, are given by (Figures 3, 4, 5)

$$\begin{aligned} q_1 &= -(l_4 \cos q_4 + l_5 \cos q_5 + l_H \cos(q_6+\gamma)) \\ q_2 &= -(l_4 \sin q_4 + l_5 \sin q_5 + l_H \sin(q_6+\gamma)). \end{aligned} \tag{39}$$

Relationships (38) can be readily solved in q_7 and q_8 in order to obtain q_7^i, q_8^i, q_7^m, and q_8^m. In this way, we have shown that the postural configurations at phase transitions are entirely defined using the 9 primary parameters introduced above.

Similarly, we want to use a minimum set of generalized velocities to complete the boundary conditions at phase transitions. We choose the hip velocity and the trunk rotation velocity in the configurations (i) and (m), as basic parameters, namely

$$\dot{q}_1^i,\ \dot{q}_2^i,\ \dot{q}_3^i,\ \dot{q}_1^m,\ \dot{q}_2^m,\ \dot{q}_3^m. \tag{40}$$

The remaining generalised velocities must be formulated as functions of the previous ones. In configuration (f), they are directly deduced from their counterparts in configuration (i) by swapping both legs:

$$\begin{aligned} &\dot{q}_1^f = \dot{q}_1^i,\ \dot{q}_2^f = \dot{q}_2^i,\ \dot{q}_3^f = \dot{q}_3^i \\ &\dot{q}_4^f = \dot{q}_7^i,\ \dot{q}_5^f = \dot{q}_8^i,\ \dot{q}_6^f = \dot{q}_9^i \\ &\dot{q}_7^f = \dot{q}_4^i,\ \dot{q}_8^f = \dot{q}_5^i,\ \dot{q}_9^f = \dot{q}_6^i \end{aligned} \tag{41}$$

A first kinematic condition, to be expressed in configuration (i), results from the fact that the rear foot is assumed to be motionless at the end of the previous SS phase. Considering planar motions, the consequence at beginning of the SS phase may be written as:

$$\mathbf{V}(O_9^i) = 0, \text{ and } \dot{q}_9^i = 0, \tag{42}$$

where $\mathbf{V}(O_9^i)$ stands for the velocity vector of point O_9^i. It can be explicitly formulated as

$$\mathbf{V}(O_9^i) = 0 \Leftrightarrow \begin{cases} \dot{q}_1^i - l_7 \dot{q}_7^i \sin(q_7^i) - l_8 \dot{q}_8^i \sin(q_8^i) = 0 \\ \dot{q}_2^i - l_7 \dot{q}_7^i \cos(q_7^i) - l_8 \dot{q}_8^i \cos(q_8^i) = 0 \end{cases}. \tag{43}$$

https://doi.org/10.1017/S0263574702004691 Published online by Cambridge University Press

Both scalar equations in (43) may be solved in $\dot{q}_7^i$ and $\dot{q}_8^i$ under the form

$$\begin{pmatrix} \dot{q}_7^i \\ \dot{q}_8^i \end{pmatrix} = \frac{1}{\sin(q_7^i - q_8^i)} \begin{pmatrix} \dfrac{\cos(q_8^i)}{l_4} & \dfrac{\sin(q_8^i)}{l_4} \\ \dfrac{-\cos(q_7^i)}{l_5} & \dfrac{-\sin(q_7^i)}{l_5} \end{pmatrix} \begin{pmatrix} \dot{q}_1^i \\ \dot{q}_2^i \end{pmatrix}. \quad (44)$$

A second kinematic condition to be used in configuration (i) is the expression of the impactless contact of the swing foot at heel-touch, which results in zero velocity of the point A_6^i (see Figure 7). This condition can be written as

$$\mathbf{V}(A_6^i) = 0 \Leftrightarrow \mathbf{J}_i \begin{pmatrix} \dot{q}_4^i \\ \dot{q}_5^i \\ \dot{q}_6^i \end{pmatrix} = \begin{pmatrix} \dot{q}_1^i \\ \dot{q}_2^i \end{pmatrix} \quad (45)$$

where

$$\mathbf{J}_i = \begin{pmatrix} l_4 \sin(q_4^i) & l_5 \sin(q_5^i) & l_H \sin(q_6^i - \gamma) \\ -l_4 \cos(q_4^i) & -l_5 \cos(q_5^i) & -l_H \cos(q_6^i - \gamma) \end{pmatrix}.$$

The algebraic system in (45) is underdetermined with respect to $\dot{q}_4^i$, $\dot{q}_5^i$, and $\dot{q}_6^i$. We have chosen to extract a minimal-norm solution using the right pseudo-inverse matrix of $\mathbf{J}_i$, namely

$$\begin{pmatrix} \dot{q}_4^i \\ \dot{q}_5^i \\ \dot{q}_6^i \end{pmatrix} = \mathbf{J}_i^+ \begin{pmatrix} \dot{q}_1^i \\ \dot{q}_2^i \end{pmatrix}. \quad (46)$$

At the end of the SS phase, we assume that the front foot becomes motionless without slamming its sole on the ground. This condition results in the following kinematic constraints

$$\mathbf{V}(O_6^m) = 0, \text{ and } \dot{q}_6^m = 0 \quad (47)$$

that are similar to constraints (42). The result of first condition in (47) can be directly deduced from (44) by changing the suffixes 7, 8 into 4, 5, respectively, namely

$$\begin{pmatrix} \dot{q}_4^m \\ \dot{q}_5^m \end{pmatrix} = \frac{1}{\sin(q_4^m - q_5^m)} \begin{pmatrix} \dfrac{\cos(q_5^m)}{l_4} & \dfrac{\sin(q_5^m)}{l_4} \\ \dfrac{-\cos(q_4^m)}{l_5} & \dfrac{-\sin(q_4^m)}{l_5} \end{pmatrix} \begin{pmatrix} \dot{q}_1^m \\ \dot{q}_2^m \end{pmatrix}. \quad (48)$$

As a last condition, we must prescribe a zero velocity of point B_9^m at toe-off. Similarly to (45), one can write

$$\mathbf{V}(B_9^m) = 0 \Leftrightarrow \mathbf{J}_m \begin{pmatrix} \dot{q}_7^m \\ \dot{q}_8^m \\ \dot{q}_9^m \end{pmatrix} = \begin{pmatrix} \dot{q}_1^m \\ \dot{q}_2^m \end{pmatrix} \quad (49)$$

with

$$\mathbf{J}_m = \begin{pmatrix} l_7 \sin(q_7^m) & l_8 \sin(q_8^m) & l_6 \sin(q_9^m) \\ -l_7 \cos(q_7^m) & -l_8 \cos(q_8^m) & -l_6 \cos(q_9^m) \end{pmatrix}.$$

As in (46), we extract a minimal-norm solution from (49) by setting

$$\begin{pmatrix} \dot{q}_7^m \\ \dot{q}_8^m \\ \dot{q}_9^m \end{pmatrix} = \mathbf{J}_m^+ \begin{pmatrix} \dot{q}_1^m \\ \dot{q}_2^m \end{pmatrix}. \quad (50)$$

Constraints (36) to (50) formulated at phase transitions show that the corresponding configurations may be characterized using only the step length, and 14 postural and velocity parameters we regroup into the following $\mathbf{x}_B$ vector

$$\mathbf{x}_B = (q_3^i, q_4^i, q_5^i, q_6^i, q_3^m, q_4^m, q_5^m, q_9^m, \dot{q}_1^i, \dot{q}_2^i, \dot{q}_3^i, \dot{q}_1^m, \dot{q}_2^m, \dot{q}_3^m)^T. \quad (51)$$

In fact, the transition configurations will be optimised through the above parameters that will be dealt with as complementary optimisation variables in the following.

4.3. Complementary constraints

The walking speed V is correlated with the step length as follows

$$V = l_S / (T_{DS} + T_{SS}) \quad (52)$$

This relationship in which we assume that V is specified, constitutes an additional equality constraint linking l_S, T_{DS} and T_{SS} considered as complementary optimisation parameters. Moreover, as we intend to generate smooth movements, we prescribe the continuity of actuating torques at gait phase transitions. Torque continuity can be ensured through gait acceleration continuity prescribed at motion phase transitions by setting

$$\ddot{\mathbf{q}}_{DS}^i = \ddot{\mathbf{q}}_{SS}^f, \ \ddot{\mathbf{q}}_{DS}^m = \ddot{\mathbf{q}}_{SS}^m \quad (53)$$

As a result, contact forces are also continuous as continuous functions of both joint velocities and accelerations.

5. PARAMETRIC OPTIMISATION

5.1. Trajectory parameters

Parametric motion optimisation can be achieved using two main approaches. The most popular one consists in representing the generalized coordinates q_is as finite linear combinations of basis functions φ_js such that

$$\forall t \in [0, T], \ q_i(t) = \sum_{j=0}^{m} a_{ij} \varphi_j(t), \qquad i = 1, \ldots, n, \quad (54)$$

where coefficients a_{ij} are intended to be dealt with as a finite set of optimisation parameters. Approximation functions φ_js may be trigonometric functions or simply polynomials such as $\varphi_j(t) = t^j$. Particularly, cubic and fourth-degree polynomials functions are used for gait trajectory optimisation.[9,10] In the first case, each q_i-trajectory is completely defined by its four position and velocity boundary conditions, whereas in the second case, only one free parameter is allowed. The

https://doi.org/10.1017/S0263574702004691 Published online by Cambridge University Press

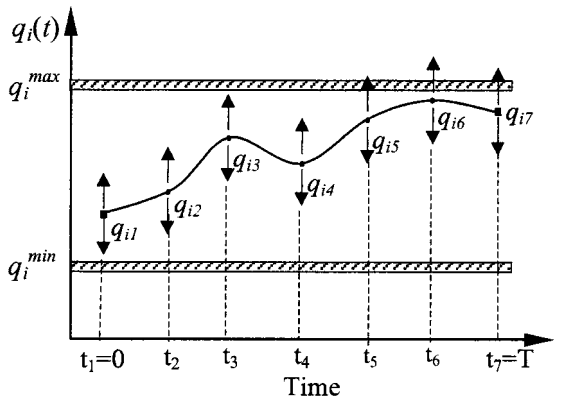

Fig. 8. Trajectory approximation using cubic-spline interpolation at knots.

search field of the optimal trajectory is then very restricted. Increasing the polynomial order m in (54) provides the q_i-trajectory with m-3 free parameters for fixed boundary conditions, and m-5 if we add acceleration boundary conditions. Nevertheless, increasing polynomial order yields undesirable oscillatory trajectories.[18,19]

In (54), $q_i(t)$ is globally approximated on the whole motion-time interval. A better approach consists in approximating q_i locally at time subintervals. In this way, one can choose directly the $q_i(t_k)$ values at connecting points t_k, or knots, as optimisation parameters (Figure 8) and approximate $q_i(t)$ between knots using polynomials, linear interpolations or cubic splines. Cubic splines represent the better choice. They are able to ensure the continuity of first and second order derivatives at knots and, unlike higher order polynomials, they allow actuating torques to have sharp variations if necessary, while avoiding undesirable oscillations. Spline coefficients are defined accounting for connecting conditions at knots. They appear as the solution of a tridiagonal linear system[20] that can be readily solved.

Let n_{DS} and n_{SS} be the number of knots introduced to optimise the DS and SS phase, respectively. Knots may be chosen uniformly distributed along the time history. In addition to the free boundary parameters shown in (51), the number of new optimisation parameters, namely the $q_i(t_k)$s, amounts to $9(n_{DS}-2)$ and $5(n_{SS}-2)$ for both DS and SS phases, respectively.

Setting

$$\mathbf{x}_{DS}=\{q_i(t_k),\ i\le n,\ t_k\in[0,\ T_{DS}]\}$$
$$\mathbf{x}_{SS}=\{q_i(t_k),\ i\le n,\ t_k\in[T_{DS},\ T_{DS}+T_{SS}]\}$$

and accounting for the free boundary parameters defining the vector $\mathbf{x}_B$ in (51), the complete set of optimisation parameters can be defined as the vector

$$\mathbf{x}=(x_1,\ \ldots,\ x_{n_p})\equiv(l_s,\ T_{DS},\ T_{SS},\ \mathbf{x}_B,\ \mathbf{x}_{DS},\ \mathbf{x}_{SS}) \qquad (55)$$

Then the interpolated generalized coordinates q_is take the form

$$i\le n,\ q_i(t)=\varphi_i(\mathbf{x},\ t) \qquad (56)$$

where φ_is are known functions in $\mathbf{x}$ and t. Finally, using the formulations (5) and (7) to express $\mathbf{u}$ in (16) and (26), one obtains $\mathbf{u}$ as a known vector-function $\mathbf{U}$ of $\mathbf{x}$ and t, namely

$$\mathbf{u}(\mathbf{q}(t),\ \dot{\mathbf{q}}(t),\ \ddot{\mathbf{q}}(t))=\mathbf{U}(\mathbf{x},\ t), \qquad (57)$$

to be used in the next section.

5.2. Performance criterion and constraints

As a biped is essentially submitted to gravity, minimizing its joint actuating torques will favour upright walking patterns. Therefore, the performance criterion we want to minimise is the integral of quadratic actuating torques as already defined in (2) and (8) (Section 2). In fact, we consider the following criterion J as the sum of two terms

$$\text{Minimise } J(\mathbf{x}),\ J(\mathbf{x})=(1-\xi)J_{DS}(\mathbf{x})+\xi J_{SS}(\mathbf{x}) \qquad (58)$$

where $\xi\in[0,\ 1]$ is a weighting factor. J_{DS} is the DS-phase criterion defined as in (18) after having changed $\mathbf{u}$ using its right-hand side expression in (57)

$$J_{DS}(\mathbf{x})=\int_0^{T_{DS}}[\mathbf{U}^T(\mathbf{x},\ t)\ \mathbf{W}\ \mathbf{U}(\mathbf{x},\ t)+\Phi(\mathbf{x},\ t)]\ dt, \qquad (59)$$

while J_{SS} has simply the structure (3), $\mathbf{u}$ being taken from (26) under the form (57), hence

$$J_{SS}(\mathbf{x})=\int_{T_{DS}}^{T_{DS}+T_{SS}}\mathbf{U}^T(\mathbf{x},\ t)\ \mathbf{W}\ \mathbf{U}(\mathbf{x},\ t)\ dt.$$

All constraints depending on the running time t defined in Section 4, excluding closure constraints (9) dealt with in (59) using the penalty function Φ defined in (16), are accounted for at known connecting times t_k. In this way, using the $\mathbf{x}$-representation of q_is and $\mathbf{u}$ in (56) and (57), they can be easily recast as constraints depending on $\mathbf{x}$ that we formally reformulate using the standard notations

$$C_j^e(\mathbf{x})=0,\ j\le n_{ec} \qquad (60)$$
$$C_k^i(\mathbf{x})\le 0,\ k\le n_{ic} \qquad (61)$$

where n_{ec} and n_{ic} stand for the number of equality and inequality constraints respectively.

We have used a Sequential Quadratic Programming (SQP) method to solve the constrained non-linear mathematical programming problem (58), (60), (61). This technique is designed to provide local minima. So, we cannot assure that a global minimum has been reached. Nevertheless, different initialisations of gait showed that the computing process converges towards the same solution if the bending constraints of the legs are accounted for, that is to say, if the bending mode of the legs is respected. Let us add that many further optimisations may benefit from initialisation starting with previously computed optimal solutions.

On the other hand, preliminary numerical tests showed that local versus global parameterisations, both using polynomial functions, could reduce by half the minimal value of the optimisation criterion.

6. NUMERICAL SIMULATIONS

Both simulations presented in this section apply to the biped robot BIP described in reference [15] and shown in Figure 9. Each leg has six actuated axis (two at ankle, one at knee and three at hip). The locomotion system is designed to generate human-like gait.

Required geometrical and inertial parameters of the robot are given in Table I. The total weight of the biped is about 107 kg.

https://doi.org/10.1017/S0263574702004691 Published online by Cambridge University Press

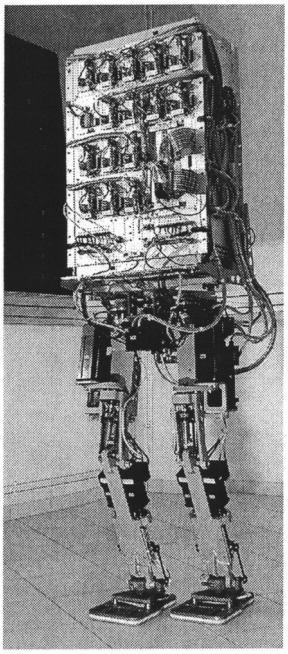

Fig. 9. View of the biped BIP (INRIA-RA, Grenoble, and LMS, University of Poitiers, France).

The ground-foot friction coefficient was set to $f=2/3$, and the weighting factor in (58) to $\xi=1/2$.

Energy expenditure was computed using the following formula:

$$W=\int_0^{T_{DS}+T_{SS}} \sum_{i=1}^{6} |\dot{\theta}_i u_i| \, dt \qquad (62)$$

where $\dot{\theta}_i$ stands for the ith-joint relative velocity.

Optimisation results were computed for two specified walking speeds.

6.1. Slow walk: V=0.4 m/s

We summarise the main optimisation results as follows:

- The criterion minimal normalized value is equal to 0.20 ($J_{DS}=0.099$, $J_{SS}=0.101$)
- The gait cycle time is equal to 1.26 *s*, 10.2% of which for the DS-phase.
- The optimal step length is equal to 0.504 *m*.
- Energy expenditure amounts to 114 *J*.
- Average power: 90 *W*
- Energy consumption per meter: 226 *J/m*

The stick diagram in Figure 10 represents the biped configurations at regular time intervals during an optimal step. The DS-phase is shown in thick lines. We notice that at midswing the biped seems to perform like a compound inverse pendulum near equilibrium, which goes with a significant deceleration.

Table I. Main mechanical parameters of the biped robot BIP.

Link	Length (m)	Mass (kg)	CoG position (m)	Moment of inertia /joint axis (kg m^2)
Foot	0.29	2.34	(0.045, 0.042)	0.07
Shin	0.41	6.11	(0.152, 0.005)	0.72
Thigh	0.41	10.9	(0.160, –0.005)	1.02
Trunk	0.60	66.11	(0.391, 0.029)	18.99

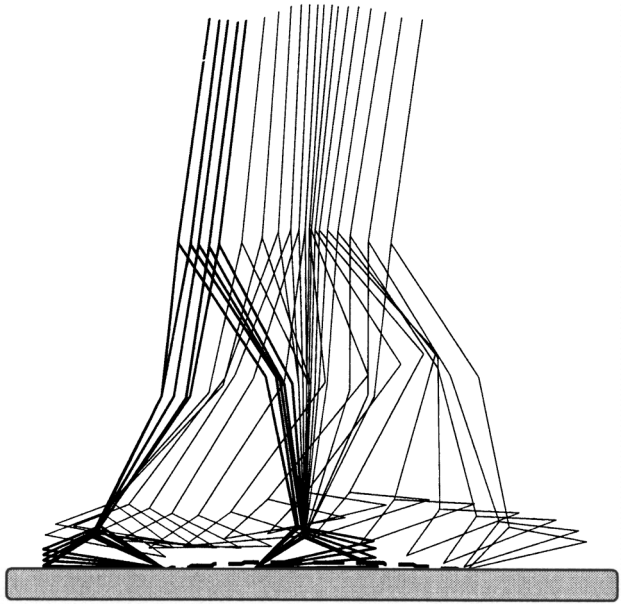

Fig. 10. Optimal gait at slow pace: V = 0.4 m/s.

Figure 11 shows the time variations of actuating torques during a gait period (two successive steps). One can notice that torque continuity is perfectly satisfied through conditions (53).

By examining torques variations shown in Figure 11 during one step, one can remark that at beginning of the SS-phase, the swing is initiated by high values of actuating torques applied at knee and ankle joints of the stance leg (u_5 and u_6, respectively). About mid-swing, during the time running from $t_1=0.35$ s to $t_2=1.05$ s, all actuating torques evolve with quite small values showing that the movement is nearly pendular. This dynamic behaviour is in agreement with experimental results reported in reference [21] indicating that there is very little activity in the swing leg muscles during human walk at normal speed, except at the beginning and the end of the SS-phase. Indeed, in our case, both legs

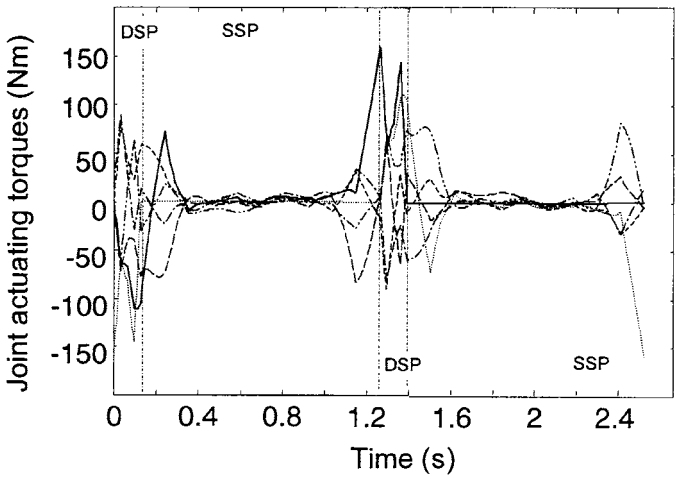

Fig. 11. Gait at slow pace: time variations of actuating torques during one gait period.

https://doi.org/10.1017/S0263574702004691 Published online by Cambridge University Press

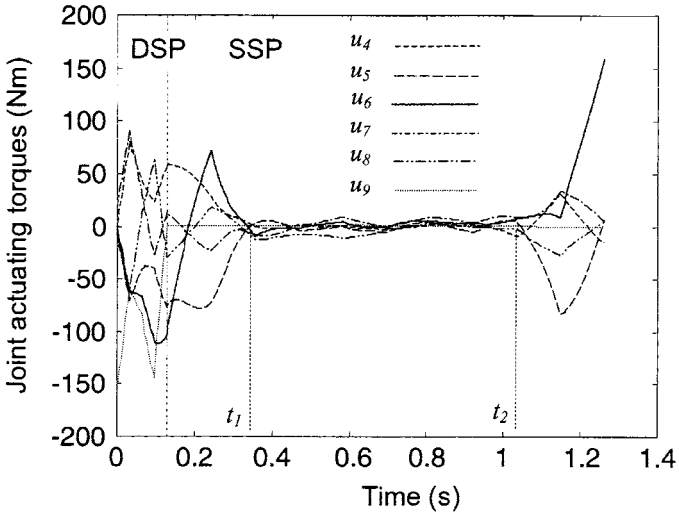

Fig. 12. Gait at slow pace: time variations of actuating torques during one cyclic step.

relax simultaneously. At the end of the SS-phase, also notice the abrupt increase of ankle torque. In addition to the others, this torque tends to slow down the swing motion in order to ensure impactless heel-touch (Fig. 12).

Figure 13 shows the time charts of reaction forces. The total normal force remains largely positive while the horizontal component keeps small values compared to the normal one, and changes its direction of action at mid-swing. Non-sliding conditions (31) and (32) are widely satisfied. During the DS-phase, the weight-transfer from the rear foot to the front foot is performed with an increase of the normal reaction force that amounts about to 180% of the biped weight.

6.2. *Fast walk: V = 1.3 m/s*

The main optimisation results are:

- Minimum criterion normalized value: 0.506 (J_{DS}=0.151, J_{SS}=0.355).
- Gait cycle time: 0.442 *s*, 11.9% for DS-phase.

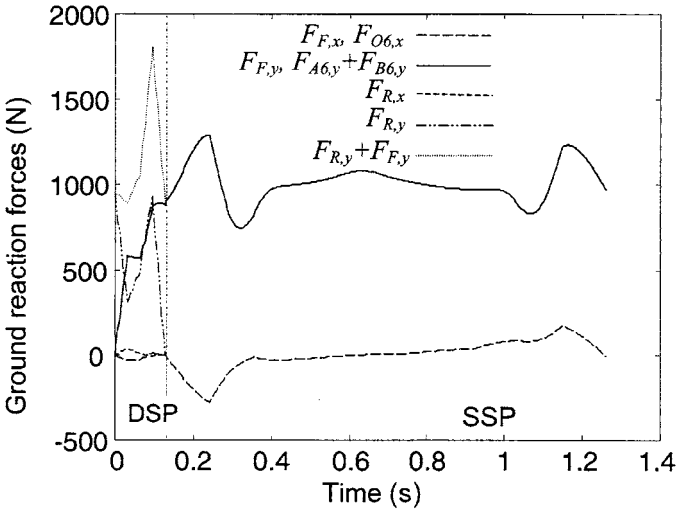

Fig. 13. Time variations of reaction forces at slow pace.

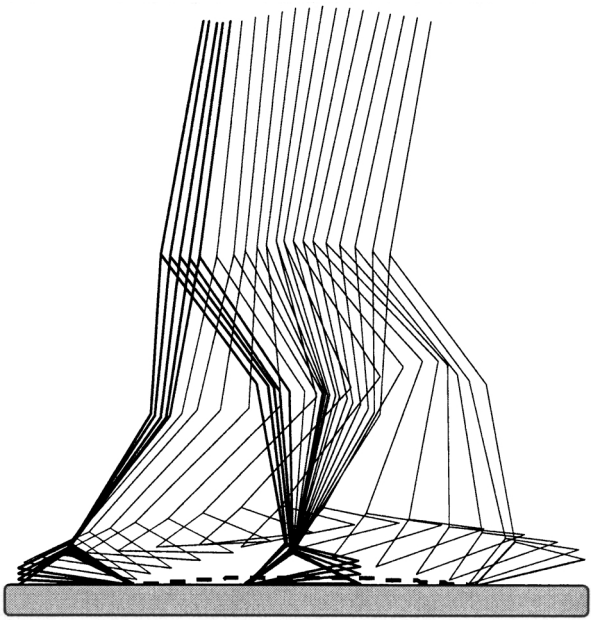

Fig. 14. Optimal gait at walk speed equal to 1.3 m/s.

- Step length: 0.575 *m*.
- Energy expenditure: 340 *J*.
- Average power: 769 *W*.
- Energy consumption per meter: 591 *J/m*.

As shown in Figure 14, the step length has increased. The motion time of the DS-phase is not quite different from its slow walk counterpart.

Also note that the stance leg remains flexed during the SS-phase. As a consequence, unlike the previous example, the knee torque (Figure 15) of the supporting leg does not decrease significantly. The pendular effect mentioned above has disappeared. Correlatively, energy consumption per meter has more than doubled.

Figure 16 shows that the biped exerts, during the DS-phase, a brief and strong impulse on the ground reaching 260% of the biped weight. On the other hand, note that the non-sliding conditions are satisfied in both phases.

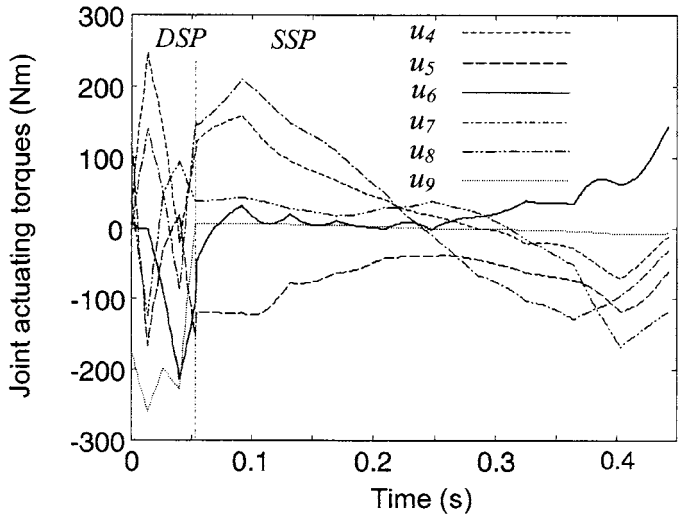

Fig. 15. Gait at fast speed: time variations of actuating torques.

https://doi.org/10.1017/S0263574702004691 Published online by Cambridge University Press

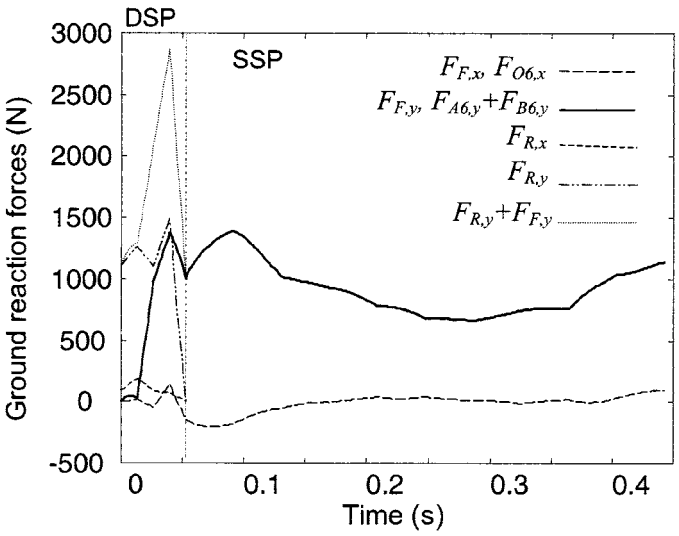

Fig. 16. Time variations of reaction forces at fast pace.

Due to the fact that the technique implemented involves a finite number of discrete optimisation parameters, it generates sub-optimal solutions. Moreover, using cubic splines ensures the continuity of joint accelerations at knots but not their differentiability, which is synonymous with jerks. These jerks are apparent in above time-charts of actuating torques and contact forces. They could be attenuated using a greater number of connecting points. It would be also possible to eliminate them using splines of higher order. However, in addition to having to deal with a greater number of optimisation variables, the consequence might be the appearance of more parasitic oscillations between knots.

7. CONCLUSION

In this paper, we developed a discrete optimisation technique aimed at generating a smooth sagittal gait cycle of a biped robot. The original optimal control problem is recast into a parameterised minimisation problem involving a finite set of discrete optimisation variables. The parameterisation concerns the generalised coordinates that are approximated using cubic splines. A complete dynamic model of the planar biped is accounted for.

A special attention is devoted to the statement of the optimisation problem considering the double-support phase during which the locomotion system works as a closed-loop mechanism. Indeterminacy of joint actuating torques is solved using a pseudo-inverse matrix technique while accounting for the ground reaction forces. Closure conditions of the kinematic loop are dealt with using a penalty method. Another important point is the specification of boundary conditions describing the transitions between the two main gait phases. From postural and kinematic constraints, we extract a maximal set of independent parameters to be optimised that characterise the transition configurations, which are consequently optimised too.

Also let us emphasise that the gait cycle is globally optimised. This approach clearly reveals that the motion time of the double-support phase can remains significant as the walk speed increases. Then the biped exerts an impelling force on the ground that intensifies with the gait speed. At the same time the step lengthens. In this way, we rediscover some basic features of human gait. Indeed, in the case of slow walk, optimisation results reveal that the biped tends to move as a gravity-driven pendulum system during a great part of the swing phase.

We have described an impactless heel-touch together with the continuity of actuating torques at phase transitions through the continuity of joint accelerations. This choice is aimed at providing the robot controller with sufficiently smooth trajectories it will be able to track efficiently. This is a first approach in generating optimal gait cycles. On the other hand, it is very likely that relaxing the continuity constraints at gait-phase transitions should help to generate a gait cycle less energy consuming. This is another objective that requires to develop a controller able to master impact and significant jerk effects on the trajectory tracking stability.

Previous results will be used to generate 3-D steps by combining lateral sway motions of the biped with the optimal sagittal gait trajectories. This combination may be carried out by simply respecting lateral bounds prescribed on the centre of pressure (or zero moment point: ZMP) trajectory in order to guarantee the dynamic equilibrium of the biped. However, the approach presented is a basis for developing a globally optimised 3-D gait. A challenging aspect of this problem lies in the dynamic complexity of a 3-D dynamic model of the biped, together with the increasing number of discrete optimisation parameters. Nevertheless, as the lateral sway motions have quite limited amplitudes with reduced velocities, the numerical conditioning of the optimisation problem should not suffer too much from this increasing complexity.

Finally, let us add that the technique presented could be used to deal with optimal motion synthesis of any actuated mechanical system having kinematic loop(s), such as parallel robots, cooperating manipulators and humans performing some athletic movements. Such systems are in most cases rooted on fixed supports, which ensures some dynamic stability. This situation will result in less constrained optimisation problems that consequently should be easier to formulate and solve.

References

1. J. Furusho & M. Masubuchi, "Control of a Dynamical Biped Locomotion System for Steady Walking," *Journal of Dynamic Systems, Measurement, and Control* **108**, 111–118 (June, 1986).
2. Q. Li, A. Takanishi & I. Kato, "Learning Control for a Biped Walking Robot with a Trunk," *Proc. of the IEEE/RSJ International Conference on Intelligent Robots and Systems*, Yokohama, Japan (1993) pp. 1771–1777.
3. K. Hirai, M. Hirose, Y. Haikawa & T. Takenaka, "The Development of Honda Humanoid Robot," *Proc. of the IEEE-ICRA*, Leuven, Belgium (1998) pp. 1321–1326.
4. Y. Fujimoto, S. Obata & A. Kawamura, "Robust Biped Walking with Active Interaction Control between Foot and Ground," *Proc. of the IEEE-ICRA*, Leuven, Belgium (1998) pp. 2030–2035.
5. M. Garcia, A. Chatterjee & A. Ruina, "Speed, Efficiency, and Stability of Small-Slope 2-D Passive Dynamic Bipedal Walking," *Proc. of the IEEE-ICRA*, Leuven, Belgium (1998) pp. 2351–2356.

https://doi.org/10.1017/S0263574702004691 Published online by Cambridge University Press

6. T. McGeer, "Passive dynamic walking," *Int. J. Robotics Research* **9**(2), 62–68 (1990).
7. M. Rostami & G. Bessonnet, "Sagittal gait of a biped robot during the single support phase. Part 1: Passive motion," *Robotica* **19**, Part 2, 163-176 (2001).
8. J. Pratt & G. Pratt, "Exploiting Natural Dynamics in the Control of a Planar Bipedal Walking Robot," *Proc. of the Thirty-Sixth Annual Allerton Conference on Communication, Control, and Computing*, Monticello, IL (1998) pp. 739–748.
9. J. Pratt & G. Pratt, "Intuitive Control of a Planar Bipedal Walking Robot," *Proc. of the IEEE-ICRA*, Leuven, Belgium (1998) pp. 2014–2021.
10. M. Rostami & G. Bessonnet, "Sagittal gait of a biped robot during the single support phase. Part 2: Optimal motion," *Robotica* **19**, Part 3, 241–253 (2001).
11. V. V. Beletskii & P. S. Chudinov, "Parametric optimisation in the problem of biped locomotion," *Mechanics of Solids* **12**, No 1, 25–35 (1977).
12. P. H. Channon, S. H. Hopkins & D.T. Pham, "Derivation of optimal walking motions for bipedal walking robot," *Robotica* **10**, Part 2, 165–172 (1992).
13. C. Chevallerau & Y. Aoustin, "Optimal reference trajectories for walking and running of a biped robot," *Robouca* **19**, Part 5, 557–569 (2001).
14. S. Chessé & G. Bessonnet, "Optimal dynamics of constrained multibody systems. Application to bipedal walking synthesis," *Proc. of the IEEE-ICRA*, Seoul, Korea (2001) pp. 2499–2505.
15. P. Sardain, M. Rostami & G. Bessonnet, "An Anthropomorphic Biped Robot: Dynamic Concepts and Technological Design," *IEEE Transactions on Systems, Man and Cybernetics* **28**(6), 823–838 (1998).
16. W. Blajer & W. Schiehlen, "Walking Without Impacts as a Motion/Force Control Problem," *ASME Journal of Dynamic Systems* **114**, 660-665 (1992).
17. G. Strang, *Linear Algebra and its Applications*, 2nd ed. (Academic Press Inc., Orlando, 1980).
18. A. Visioli, "Trajectory planning of robot manipulators by using algebraic and trigonometric splines," *Robotica* **18**, Part 6, 611–631 (2000).
19. T. Saidouni & G. Bessonnet, "Gait trajectory optimization using approximation functions," *Proc. of the 5th International Conference on Climbing and Walking Robots*, Paris, France (2002) pp. 709–716.
20. J. Stoer & R. Bulirsch, *Introduction to Numerical Analysis* (Springer-Verlag, New York, 1980).
21. T. A. McMahon, "Mechanics of locomotion," *Int. Journal of Robotics Research* **3**(2), 4–28 (1984).

https://doi.org/10.1017/S0263574702004691 Published online by Cambridge University Press